Adsorption of volatile organic compounds in porous metal–organic frameworks functionalized by polyoxometalates

Feng-Ji Ma, Shu-Xia Liu*, Da-Dong Liang, Guo-Jian Ren, Feng Wei, Ya-Guang Chen, Zhong-Min Su*

Key Laboratory of Polyoxometalates Science of the Ministry of Education, College of Chemistry, Northeast Normal University, Changchun 130024, China

ABSTRACT

The functionalization of porous metal–organic frameworks ($Cu_3(BTC)_2$) was achieved by incorporating Keggin-type polyoxometalates (POMs), and further optimized via alkali metal ion-exchange. In addition to thermal gravimetric analysis, IR, single-crystal X-ray diffraction, and powder X-ray diffraction, the adsorption properties were characterized by N_2 and volatile organic compounds (VOCs) adsorption measurements, including short-chain alcohols ($C < 4$), cyclohexane, benzene, and toluene. The adsorption enthalpies estimated by the modified Clausius–Clapeyron equation provided insight into the impact of POMs and alkali metal cations on the adsorption of VOCs. The introduction of POMs not only improved the stability, but also brought the increase of adsorption capacity by strengthening the interaction with gas molecules. Furthermore, the exchanged alkali metal cations acted as active sites to interact with adsorbates and enhanced the adsorption of VOCs.

1. Introduction

Releases, intentional or not, of volatile organic compounds (VOCs) may affect the environment or human health [1]. Accordingly, continuous research is required to develop more efficient technologies or materials to reduce the emissions of VOCs. Methods such as condensation, adsorption, catalytic oxidation, and incineration have been employed for abatement of VOCs. Adsorption as a reliable method is widely used because it provides an economical way to remove VOCs from a wide range of gaseous streams [2–4].

Various materials such as activated carbon, alumina, silica gel, and zeolite show a high specific area for the adsorption of VOCs. It is well known that their different adsorption properties depend on both the chemical composition and the unique nature of the materials. Recently, a new class of porous materials known as metal–organic frameworks (MOFs) [5] has received remarkable attention. These materials are composed of metal ions linked together by organic ligands, yielding a wide range of chemical behaviors: catalysis [6], ion-exchange [7], magnetism [8], and drug delivery [9]. With exceptionally high surface areas and chemically-tunable structures, MOFs are ideally suited for the adsorption of gases and separation of gas mixtures [10–13], and have also been studied for the use of VOCs adsorption [14].

An effective approach to optimize MOFs for more specialized applications is to functionalize MOFs. The various and tunable structures of MOFs would allow to integrate other multifunctional molecules for functionalization. Polyoxometalates (POMs) as a kind of

promising material have received increasing attention, due to their structural diversities and remarkable properties [15,16]. As versatile guests, POMs have been incorporated into MOFs to construct novel hybrid materials [17–20]. Recently, we employed this strategy to achieve the functionalization of MOFs. By encapsulating Keggin-type POMs into the nanosized spaces of porous $Cu_3(BTC)_2$ [21] (HKUST-1, BTC=1, 3, 5-benzenetricarboxylate) MOFs host, we presented a series of hybrid materials based on porous MOFs and POMs (shorten as PMOFs/POMs) for targeted application. Among them, NENU-3 $((C_4H_{12}N)_2[Cu_{12}(BTC)_8 \cdot 12H_2O][HPW_{12}O_{40}] \cdot 25H_2O)$ as heterogeneous catalyst showed high catalytic activity in the ester hydrolysis [22]. We further modified the inclusion state of these materials though ion-exchange and studied the H_2 adsorption properties [23]. Furthermore, we utilized POMs as templates and obtained a novel PMOF/POM with sodalite topology network. As a reasonable candidate for eliminating nerve gas, it not only displayed good adsorption behavior, but also realized the facile and effective decomposition of nerve gas mimic [24]. Herein, we report another K^+-exchanged PMOF/POM, $K_2[Cu_{12}(BTC)_8 \cdot 12H_2O][HPW_{12}O_{40}] \cdot 28H_2O$ (NENU-28), and systematically investigate the effect of POMs and alkali metal cations for the VOCs adsorption, including short-chain alcohols ($C < 4$), cyclohexane, benzene, and toluene.

2. Experimental

2.1. Materials and measurements

All chemicals were obtained commercially and used without additional purification. Elemental analyses (C, H, and N) were

---

* Corresponding authors. Fax: +86 43185099328.
  E-mail address: liusx@nenu.edu.cn (S.-X. Liu).

performed on a Perkin-Elmer 2400 CHN elemental analyzer, and analyze for K was carried out on a PLASMA-SPEC(I) Inductive Coupled Plasma atomic emission spectrometer. IR spectra were recorded in the range 400–4000 cm^{-1} on an Alpha Centaurt FT/IR spectrophotometer using KBr pellets. Thermal gravimetric analysis (TGA) was performed on a Perkin-Elmer TGA7 instrument in flowing N$_2$ with a heating rate of 10 °C min^{-1}. Powder X-ray diffraction (PXRD) measurements were performed on a Rigaku D/MAX-3 instrument with Cu $K\alpha$ radiation in the angular range $2\theta = 3$–$60°$ at 293 K.

2.2. Synthesis

K$_2$[Cu$_{12}$(*BTC*)$_8$H$_2$O$_n$][HPW$_{12}$O$_{40}$] (NENU-28), *Method* 1: crystals of as-synthesized NENU-3 ((C$_4$H$_{12}$N)$_2$[Cu$_{12}$(*BTC*)$_8 \cdot$ 12H$_2$O] [HPW$_{12}$O$_{40}$] $\cdot$ 25H$_2$O) [22] (2.0 g) were immersed in 100 ml saturated solution of KCl. The crystals were soaked for a week, and the KCl solution was refreshed everyday. The completely K$^+$-exchanged crystals of NENU-28 were obtained and washed with distilled water several times to remove residual free KCl. *Method* 2: the as-synthesized crystals of NENU-3 (2.0 g) were evacuated under dynamic vacuum ($\sim 10^{-6}$ mbar) at 150 °C for 12 h, then immersed in 100 ml saturated solution of KCl for 24 h. The KCl solution was refreshed once in the interim. The completely K$^+$-exchanged crystals of NENU-28 were isolated and washed with distilled water several times. Both the methods described above resulted in the same product NENU-28. Yield 1.96 g (98%). Elemental Anal. Calcd (Found %) for C$_{72}$H$_{105}$O$_{128}$K$_2$Cu$_{12}$PW$_{12}$: C, 14.18 (14.02); H, 1.72 (1.81); N, 0.00 (0.00). IR (KBr, cm^{-1}): 1894, 1648, 1457, 1374, 1123, 1082, 978, 895, 822, 749, 738, 488.

2.3. X-ray crystallography

Single-crystal diffractometry was conducted on a Bruker Smart Apex CCD diffractometer with Mo $K\alpha$ monochromated radiation ($\lambda = 0.71073$ Å) at room temperature. The linear absorption coefficients, scattering factors for the atoms, and anomalous dispersion corrections were taken from the International Tables for X-Ray Crystallography [25]. Empirical absorption corrections were applied. The structures were solved using the direct method and refined through the full-matrix least-squares method on F^2 using SHELXS-97 [26]. Anisotropic thermal parameters were used to refine all non-hydrogen atoms. The hydrogen atoms attached to carbon positions were placed in geometrically calculated positions. The crystallization water molecules were estimated by thermogravimetry, and only partial oxygen atoms of water molecules were achieved with the X-ray structure analysis. The most important crystallographic data are summarized in Table 1.

2.4. Adsorption measurements

Adsorption measurements were measured with a Hiden Isochema Intelligent Gravimetric Analyzer (IGA-100B). The sample ($\sim$100 mg) was outgassed to a constant weight at 473 K under a high vacuum ($< 10^{-6}$ mbar) prior to measurements of the isotherms. High purity N$_2$ (99.999%) were used for N$_2$ adsorption measurements at 77 K. The saturated vapor pressures of the sorbents at 298 K were shown in parentheses: methanol (168.08 mbar), ethanol (78.96 mbar), 1-propanol (27.59 mbar), 2-propanol (60.21 mbar), cyclohexane (131.27 mbar), benzene (126.61 mbar), and toluene (37.89 mbar). The temperature at 77 K was maintained with liquid nitrogen and the temperatures at 298 K and 308 K were maintained with constant temperature water bath. The DA pore size distribution analysis was calculated by the IGASWIN software of the IGA system.

Table 1
Crystal data and structure refinement for NENU-28.

Empirical formula	C$_{288}$H$_{96}$K$_8$Cu$_{48}$P$_4$W$_{48}$O$_{420}$
fw	22617.19
Crystal system	Cubic
Space group	$Fm\bar{3}m$
a (Å)	26.4022(13)
V (Å^3)	18404.3(16)
Z	1
F (000)	10353.8
Dc (g/cm^3)	2.041
abs coeff. (mm^{-1})	8.961
Reflns collected	28,316
Independent reflns	1197
θ range (deg.)	1.54–28.23
GOF on F^2	1.100
R_{int}	0.0455
R_1 [$I > 2\sigma(I)$]^a	0.0361
wR_2 (all data)^b	0.1236

^{a} $R_1 = \sum | |F_o| - |F_c| | / \sum |F_o|$,
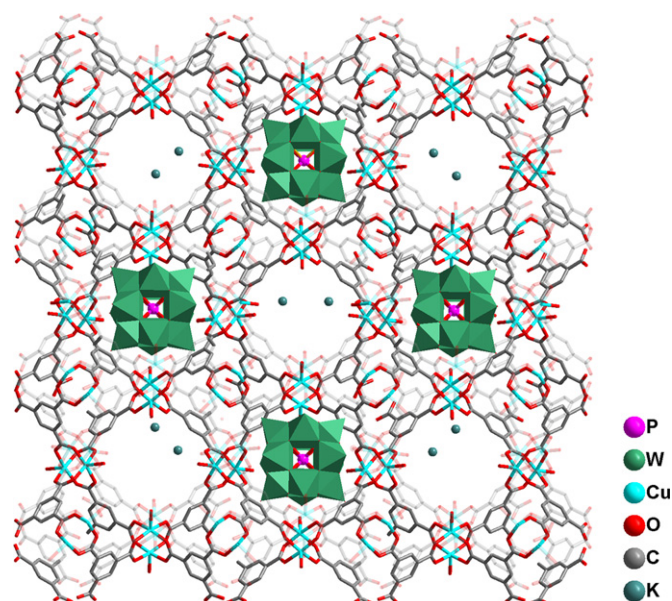^{b} $wR_2 = \{\sum[w(F_o^2 - F_c^2)^2] / \sum[w(F_o^2)^2]\}^{1/2}$.

Fig. 1. Structure illustrated for NENU-28 along the [001].

3. Results and discussion

3.1. Crystal structure

Single crystal X-ray structural analysis revealed that the overall structure of NENU-28 was not altered after the ion exchange process. As shown in Fig. 1, it presents two types of pores. The larger pore (ca. 13 Å) contains the POMs anions. And K ions are in the smaller pore (ca. 10 Å). The difference between NENU-3 and NENU-28 is that the counterions (CH$_3$)$_4$N$^+$ are exchanged by K$^+$. While the K$^+$ can be regarded as open coordination sites to access other guest molecules, such as the adsorbed molecules. The theoretical total accessible volume of NENU-28 after removal of water molecules is 23.1%, using the PLATON [27] routine. The value is a little lower than NENU-3 (29.8%).

3.2. Stability and structural integrity

TGA indicates a weight loss of 12.4% (calcd 11.8%) at 200 °C, which corresponds to the loss of all the water molecules (Figure S2). The solid is thermally stable up to 300 °C, which is higher

than the $Cu_3(BTC)_2$ framework (~ 240 °C). The improvement of thermal stability could be assigned to the encapsulation of POMs. The PXRD pattern of NENU-28 matches the simulated pattern from the single crystal X-ray data (Figure S4), implying that the bulk sample is same as the single crystal and possesses high purity. Subsequent adsorption measurements also show that NENU-28 has high stability (Figure S5). The functionalization of MOFs by incorporating POMs enhances the stability of the material, more importantly, shows a positive implication for more application, such as adsorption and catalysis.

A complete exchange of the $(CH_3)_4N^+$ by K^+ was observed without losing the structural integrity. The ion exchange process monitored by inductive coupled plasma (ICP) confirmed the facile exchange from $(CH_3)_4N^+$ to K^+: about 20% of $(CH_3)_4N^+$ were substituted by K^+ within 24 h; after 72 h, K^+ had replaced half equivalent of $(CH_3)_4N^+$ from the framework; a week later, complete exchange finished. The elimination of $(CH_3)_4N^+$ was also indicated by the disappearance of the C–H vibrating peak in the IR spectrum (Figure S3). Moreover, the C, H, and N elemental analyses further indicated that no N was present in NENU-28.

3.3. N_2 adsorption studies

The permanent porosities were evaluated by N_2 adsorption at 77 K. The sample of NENU-28 was heated at 200 °C under vacuum for 12 h to give the desolvated NENU-28a ($K_2[Cu_{12}(BTC)_8][HPW_{12}O_{40}]$), which was employed to study the porosity and adsorption properties. As shown in Fig. 2, both N_2 isotherms of NENU-28 and NENU-3 show typical Type-I adsorption behavior. The N_2 adsorption increases abruptly at the start of the experiment and reaches a plateau at $P/P_0 = 0.05$, indicating the presence of the microporous structures [28]. NENU-28 adsorbs 163 cm³ (STP) g⁻¹ of N_2 at 77 K and 1 atm, and this value is higher than that of NENU-3 (126 cm³ (STP) g⁻¹). Brunauer–Emmett–Teller (BET) surface areas for NENU-3 and NENU-28 were estimated as 390 and 470 m² g⁻¹, respectively. The data of N_2 adsorption suggest that the adsorption capacity of NENU-28 increases by ca 20% on K^+-exchange. Applying Dubinin–Astakhov (DA) analysis [29] to the isotherm data shows that the pore sizes are distributed narrowly around 8.7 Å for NENU-3 and 7.3 Å for NENU-28 (Fig. 2).

3.4. VOCs adsorption studies

We choose methanol, ethanol, 1-propanol, 2-propanol, cyclohexane, benzene, and toluene for VOCs adsorption studies. The adsorption isotherms of methanol at 298 K show a corresponding improvement in storage capacity on K^+-exchanged NENU-28 (Fig. 3). The adsorption amounts of methanol are 6.70 mmol g⁻¹ and 5.89 mmol g⁻¹ for NENU-28 and NENU-3, respectively. They
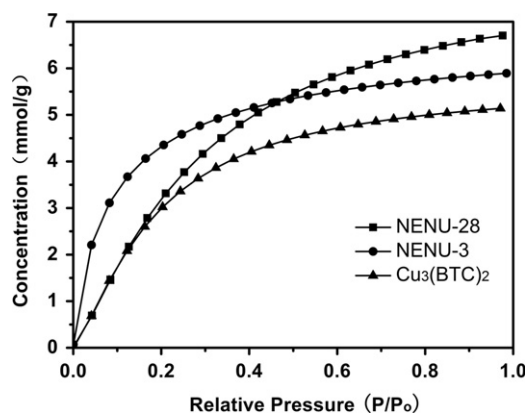

Fig. 2. N_2 adsorption isotherms at 77 K and pore size distributions.

Fig. 3. Methanol adsorption isotherms at 298 K for NENU-28, NENU-3, and $Cu_3(BTC)_2$.

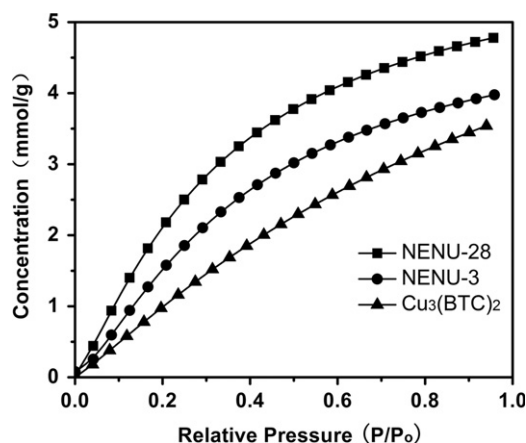**Fig. 4.** Ethanol adsorption isotherms at 298 K for NENU-28, NENU-3, and $Cu_3(BTC)_2$.

are equivalent to the adsorption of 37.52 and 32.39 methanol molecules per formula unit, respectively [30]. Comparing with host framework $Cu_3(BTC)_2$ (5.14 mmol g⁻¹, 14.36 methanol molecules per formula unit), POMs-functionalized porous MOFs exhibit markedly increased adsorption capacity for methanol.

Fig. 4 shows the adsorption isotherms of ethanol for NENU-28, NENU-3, and $Cu_3(BTC)_2$ at 298 K. The adsorption amounts of ethanol increase gradually with the increase of relative pressure. Similar to methanol adsorption, NENU-28 has a higher adsorption capacity for ethanol (4.78 mmol g⁻¹, 26.77 ethanol molecules per formula unit) than NENU-3 (3.97 mmol g⁻¹, 21.84 ethanol molecules per formula unit) at 298 K. And these values are higher than that of $Cu_3(BTC)_2$ (3.54 mmol g⁻¹, 9.89 ethanol molecules per formula unit), though the BET surface area of $Cu_3(BTC)_2$ is higher [31] (Table 2). In fact, because of the larger molecular weights of POM and the higher surface area of parent MOF, the adsorption amount of methanol and ethanol on a mass basis or on a volume basis for $Cu_3(BTC)_2$ is higher than PMOFs/POMs. However, POMs cannot be ignored for their contribution to the adsorption. The results of the above suggest that POMs-functionalized PMOFs/POMs adsorb greater amount of methanol and ethanol molecules per formula unit. In other words, the presence of POMs is beneficial to the enhancement of adsorption. The interaction between adsorbed molecules and the O atoms of the POMs may allow the increase of uptake by hydrogen bonding. Furthermore, it is found that the exchange of alkali metal cations may also bring on an increase in the adsorption capacity via comparing the data of NENU-28 and NENU-3. And the results of Li^+ exchanged NENU-29 ($Li_2[Cu_{12}(BTC)_8 \cdot 12H_2O][HPW_{12}O_{40}] \cdot 27H_2O$) [23] confirmed this
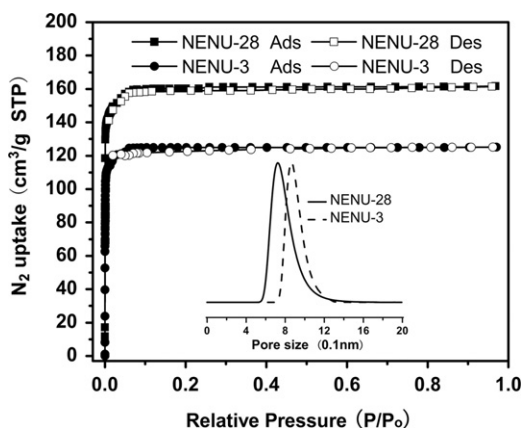
Table 2
Adsorption properties of NENU-28, NENU-3, NENU-29, and Cu$_3$(BTC)$_2$.

	SA$_{BET}$[a]	Methanol			Ethanol			1-propanol[d]	2-propanol	Cyclohexane	Benzene	Toluene
		298 K[b]	308 K	ΔH_{ads}[c]	298 K	308 K	ΔH_{ads}					
NENU-28	470	6.70	5.92	43.66	4.78	4.17	40.64	3.62	2.69	1.70	3.42	2.89
NENU-29	466	6.28	5.58	40.57	4.25	3.87	38.52	2.98	1.91	1.64	3.38	2.78
NENU-3	405	5.89	4.74	37.55	3.97	3.38	36.28	0.61	0.41	1.58	3.29	2.65
Cu$_3$(BTC)$_2$	1507	5.14	4.04	35.27	3.54	2.92	34.51	–	–	1.48	3.21	2.54

[a] Obtained from the N$_2$ isotherms at 77 K, m^2 g^{-1}.
[b] mmol g^{-1}.
[c] kJ mol^{-1}.
[d] at 298 K, mmol g^{-1}.
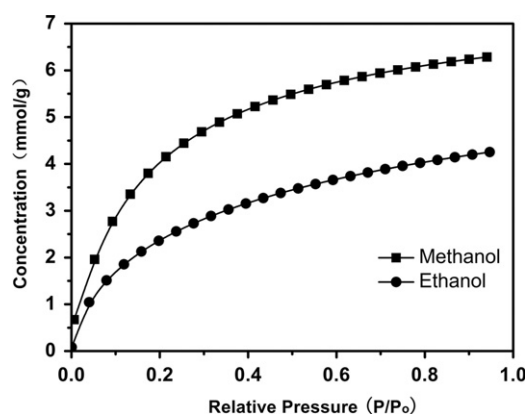
Fig. 5. Methanol and ethanol adsorption isotherms at 298 K for NENU-29.

inference. As expected, NENU-29 adsorbs more methanol and ethanol than NENU-3 (Fig. 5). It exhibits methanol uptake of 6.28 mmol g^{-1} (33.28 methanol molecules per formula unit) and ethanol uptake of 4.25 mmol g^{-1} (22.53 ethanol molecules per formula unit), respectively. It is indicated that alkali metal cations indeed contribute favorably to the enhancement of adsorption. As open active sites, alkali metal cations are accessible to the adsorbed molecules and interact with them.

To further predict the adsorption capacity, we estimated the adsorption enthalpy obtained from isotherms, using the experience of gas adsorption for reference [23,32–34]. Second set of adsorption isotherms were measured at 308 K (Fig. 6) and the adsorption enthalpies were calculated using the modified Clausius–Clapeyron equation [35]. The adsorption isotherms were fitted by the Langmuir–Freundlich equation (see the Supporting Information) [36]. Fig. 7a shows the methanol adsorption enthalpies for Cu$_3$(BTC)$_2$ (35.27 kJ mol^{-1}), NENU-3 (37.55 kJ mol^{-1}), NENU-29 (40.57 kJ mol^{-1}) and NENU-28 (43.66 kJ mol^{-1}). The adsorption enthalpies are found to be in the order: NENU-28 > NENU-29 > NENU-3 > Cu$_3$(BTC)$_2$ (Table 2). In addition, the ethanol adsorption enthalpies show the similar result (Fig. 7b). The hydrogen bonding interactions provided by POMs also increase the adsorption. Simultaneity, the exchanged alkali metal cations enhance the binding affinity between the adsorbates and adsorbent, which may be the ion–dipole electrostatic interactions. The alkali metal cations may attract the partially negative end of the vapor molecules, and further increase the adsorption of the vapor. The mechanistic details of the interactions are currently poorly understood, yet these results demonstrate that the POMs and alkali metal cations play crucial roles in enhancing VOCs adsorption.
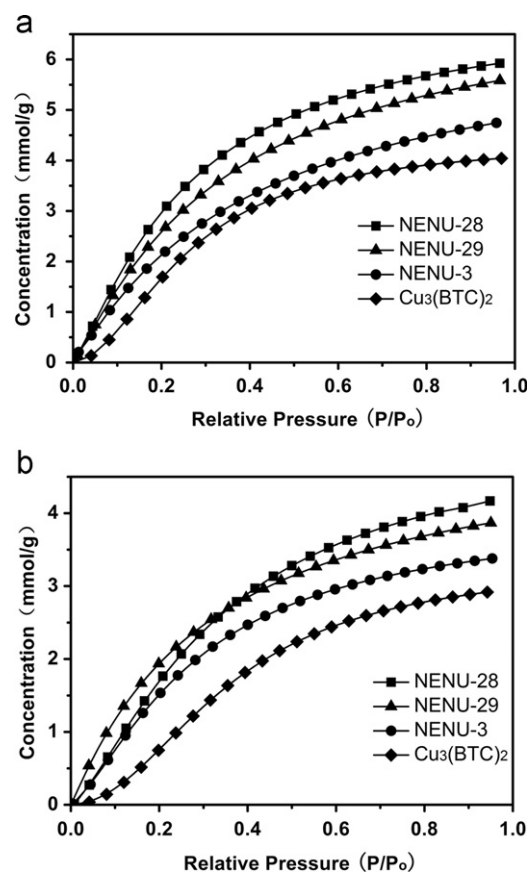
Fig. 6. Methanol (a) and ethanol (b) adsorption isotherms at 308 K for NENU-28, NENU-29, NENU-3, and Cu$_3$(BTC)$_2$.

Subsequent adsorption measurements of 1-propanol and 2-propanol at 298 K further confirm the impact of alkali metal cations on the VOCs adsorption. As Fig. 8 shown, it is worth noting that NENU-3 hardly adsorbs 1-propanol (0.61 mmol g^{-1}) and 2-propanol (0.41 mmol g^{-1}) at 298 K. In comparison, NENU-28 adsorbs 1-propanol 3.62 mmol g^{-1} (20.27 1-propanol molecules per formula unit) and 2-propanol 2.69 mmol g^{-1} (15.06 2-propanol molecules per formula unit), respectively; NENU-29 adsorbs 1-propanol 2.98 mmol g^{-1} (15.79 1-propanol molecules per formula unit) and 2-propanol 1.91 mmol g^{-1} (10.12 2-propanol molecules per formula unit), respectively. For NENU-3, the adsorbed molecules bind with the framework and POMs guests by hydrogen bondings. However, alkali metal exchanged NENU-28 and NENU-29 afford an extra interaction with the adsorbed molecules, which leads to significant enhancement of adsorption.
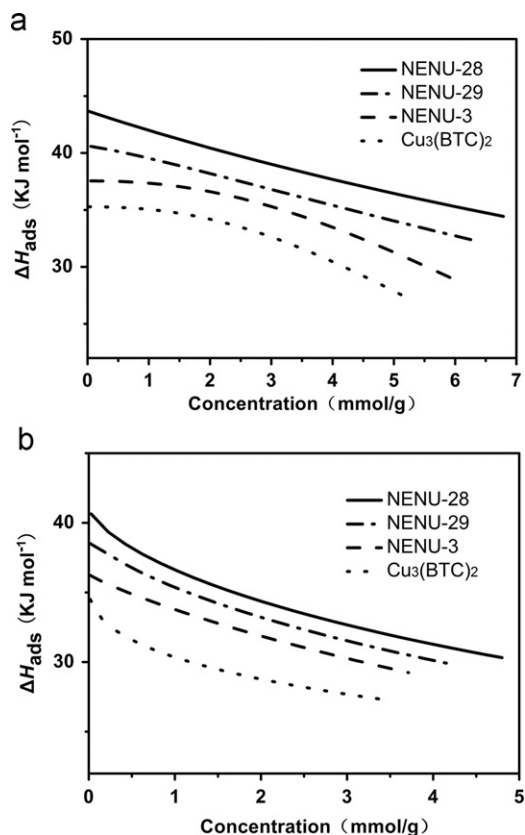
Fig. 7. Methanol (a) and ethanol (b) adsorption enthalpies for NENU-28, NENU-29, NENU-3, and Cu$_3$(BTC)$_2$.
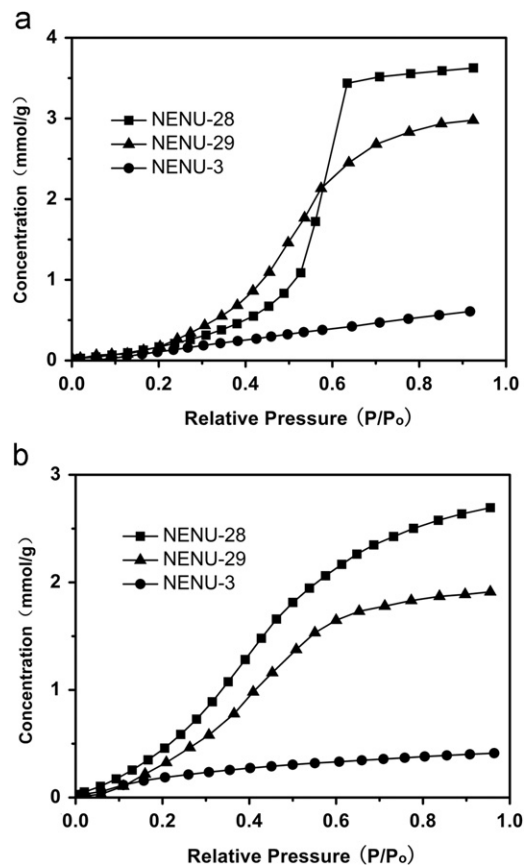

Fig. 8. 1-propanol (a) and 2-propanol (b) adsorption isotherms at 298 K for NENU-28, NENU-29, and NENU-3.

In combination with the results mentioned above, it is remarkable that K$^+$-exchanged NENU-28 displayed the best adsorption for VOCs molecules. It may be attributed to the larger radiu of K$^+$, which makes it easy to access and interact with the adsorbed molecules. The ion–dipole attractions become stronger as the magnitude of ions increase. Thus, the larger K$^+$ makes stronger interactions with the vapor molecules than Li$^+$ to increase the adsorption. Anyway, it is highlighted that the presence of alkali metal cations provides strong interactions to increase the adsorption capacity.

We further assessed the validity of PMOFs/POMs for adsorption of the less polar VOCs by the adsorption measurements of cyclohexane, benzene and toluene at 298 K (Fig. 9). The results are consistent with the findings of before. The interactions between the adsorbates and adsorbent became weaker as the polarity decreased, and the gap of adsorption capacities has narrowed. Yet, NENU-28 still exhibits the best adsorption behavior (Table 2). In the low P/P_0 region ($P/P_0 < 0.2$), the rapid adsorption for benzene and toluene indicates the presence of
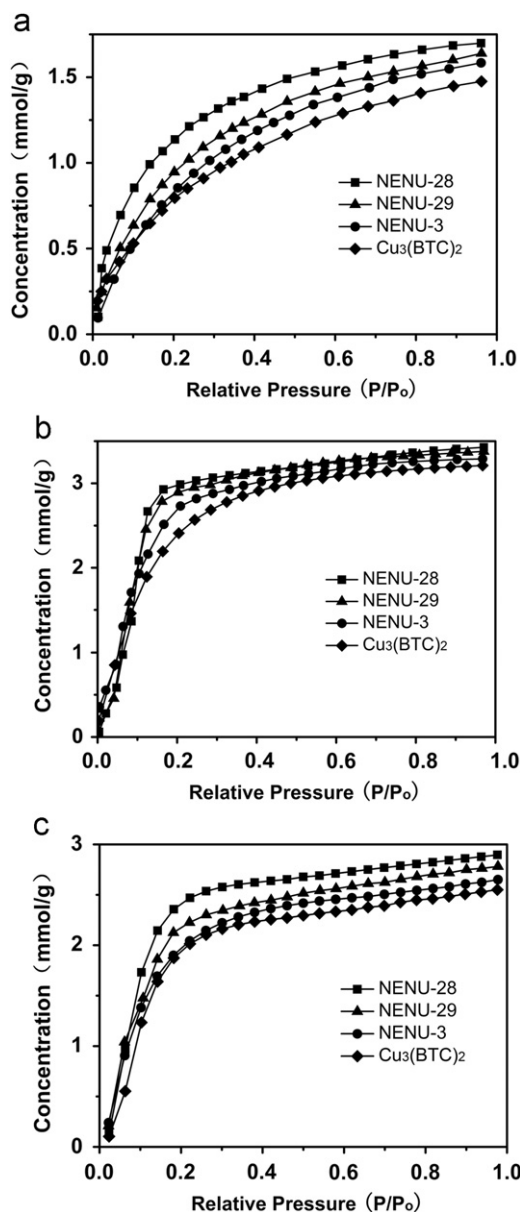

Fig. 9. Cyclohexane (a), benzene (b), and toluene (c) adsorption isotherms at 298 K for NENU-28, NENU-29, NENU-3, and Cu$_3$(BTC)$_2$.

a strong guest–host interaction. In contrast, the adsorption of cyclohexane increases gradually along with the increasing relative pressure, owing to the relatively weak interaction with the framework. The strength of interaction between guest molecules and host framework may cause the differences of adsorption isotherms. Benzene and toluene are likely to participate in π–π interactions with the ligands in the framework, resulting stronger interactions. Contrarily, cyclohexane is inert in the intermolecular interaction with a slowing uptaken [37]. According to the tests on cyclohexane, benzene, and toluene, NENU-28 acts effectively for the adsorption of VOCs.

4. Conclusion

In conclusion, we have functionalized porous MOFs by encapsulating Keggin-type POMs and further modified the inclusion state via ion exchange. By initiating a systematic evaluation, we have demonstrated that POMs and alkali metal cations played important roles for increasing the adsorption capacity of MOFs. The extensive hydrogen bondings between adsorbed molecules and POMs guests as well as the strong interaction between the alkali metal cations and adsorbates both increase the adsorption. As a new class of porous materials, PMOFs/POMs display the potential application in the adsorption of VOCs. In virtue of the significant catalytic activities of POMs, these materials may be further used in VOCs purge. Our future efforts will focus on preparing new PMOFs/POMs by governing the exchange purposefully and exploring their use for more applications.

Supplementary data

CCDC-754629 contains crystallographic data. The data can be obtained free of charge from the Cambridge Crystallographic Data Centre via http://www.ccdc.cam.ac.uk/data_request/cif. Supplementary data associated with this article, including TG curve, IR spectra, PXRD data, and details of the estimation of adsorption enthalpy, can be found in the online version, at doi:10.1016/j.jssc.2011.09.002.

Acknowledgments

Appendix A. Supporting information

Supplementary data associated with this article can be found in the online version at doi:10.1016/j.jssc.2011.09.002.

References

[1] R.E. Hester, R.M. Harrison (Eds.), Volatile Organic Compounds in the Atmosphere, the Royal Society of Chemistry, Cambridge, 1995.
[2] K. Katsunori, K. Shiori, K. Nobuyuki, T. Makoto, Langmuir 23 (2007) 3095–3102.
[3] J. Ikram, F. Sophie, B. Mourad, B. Samir, Chem. Geol. 275 (2010) 1–8.
[4] D.P. Serrano, G. Calleja, J.A. Botas, F.J. Gutierrez, Ind. Eng. Chem. Res. 43 (2004) 7010–7018.
[5] O.M. Yaghi, H. Li, C. Davis, D. Richardson, T.L. Groy, Acc. Chem. Res. 31 (1998) 474–484.
[6] R. Zou, H. Sakurai, Q. Xu, Angew. Chem. Int. Ed. 45 (2006) 2542–2546.
[7] K.L Mulfort, J.T. Hupp, J. Am. Chem. Soc. 129 (2007) 9604–9605.
[8] Y.Z. Zheng, M.L. Tong, W.X. Zhang, X.M. Chen, Angew. Chem. Int. Ed. 45 (2006) 6310–6314.
[9] J. An, S.J. Geib, N.L. Rosi, J. Am. Chem. Soc. 131 (2009) 8376–8377.
[10] M. Dinc, J.R. Long, Angew. Chem. Int. Ed. 46 (2007) 1419–1422.
[11] A.G. Wong-Foy, A.J. Matzger, O.M. Yaghi, J. Am. Chem. Soc. 128 (2006) 3494–3495.
[12] S. Shimomura, M. Higuchi., R. Matsuda, K. Yoneda, Y. Hijikata, Y. Kubota, Y. Mita, J. Kim, M. Takata, S. Kitagawa, Nat. Chem. 2 (2010) 633–637.
[13] P.L. Llewellyn, S. Bourrelly, C. Serre, Y. Filinchuk, G. Férey, Angew. Chem. Int. Ed. 45 (2006) 7751–7754.
[14] M.T. Luebbers, T. Wu, L. Shen, R.I. Masel, Langmuir 26 (2010) 11319–11329.
[15] D.L. Long, R. Tsunashima, L. Cronin, Angew. Chem. Int. Ed. 49 (2010) 1736–1758.
[16] C.L. Hill, Special issue on polyoxometalates, Chem. Rev. 98 (1998) 1–387.
[17] X.F. Kuang, X.Y. Wu, R.M. Yu, J.P. Donahue, J.S. Huang, C.Z. Lu, Nat. Chem. 2 (2010) 461–465.
[18] X.Y. Liu, Y.Y Jia, Y.F. Zhang, R.D. Huang, Eur. J. Inorg. Chem. 25 (2010) 4027–4033.
[19] X.Y. Zhao, D.D. Liang, S.X. Liu, C.Y. Sun, R.G. Cao, C.Y. Gao, Y.H. Ren, Z.M. Su, Inorg. Chem. 47 (2008) 7133–7138.
[20] S.X. Liu, L.H. Xie, B. Gao, C.D. Zhang, C.Y. Sun, D.H. Li, Z.M. Su, Chem. Commun. 40 (2005) 5023–5025.
[21] S.S.Y. Chui, S.M.F. Lo, J.P.H. Charmant, A.G. Orpen, L.D. Williams, Science 283 (1999) 1148–1150.
[22] C.Y. Sun, S.X. Liu, D.D. Liang, K.Z. Shao, Y.H. Ren, Z.M. Su, J. Am. Chem. Soc. 131 (2009) 1883–1888.
[23] F.J. Ma, S.X. Liu, D.D Liang, G.J. Ren, C.D. Zhang, F. Wei, Z.M. Su, Eur. J. Inorg. Chem. 24 (2010) 3756–3761.
[24] F.J. Ma, S.X. Liu, C.Y. Sun, D.D Liang, G.J. Ren, F. Wei, Y.G. Chen, Z.M. Su, J. Am. Chem. Soc. 133 (2011) 4178–4181.
[25] N.F.M. Henry, K. Lonsdale (Eds.), International Tables for X-ray Crystallography, Kynoch Press, Birmingham, 1952.
[26] G.M. Sheldrick, SHELXS-97: Programs for Crystal Structure Solution, University of Göttingen, Göttingen, 1997.
[27] A.L. Spek, J. Appl. Crystallogr. 36 (2003) 7–13.
[28] F. Rouquerol, J. Roquerol, K. Sing, Adsorption by Powders and Porous Solids, Academic Press, London, 1999.
[29] S.J. Gregg, K.S.W. Sing, Adsorption, Surface Area and Porosity, Academic Press, London, 1982.
[30] We defined all the formula units as Cu12 congruously for the comparisons of adsorption: $H_2[Cu_{12}(BTC)_8][HPW_{12}O_{40}]$ for NENU-3, $K_2[Cu_{12}(BTC)_8][HPW_{12}O_{40}]$ for NENU-28, $Li_2[Cu_{12}(BTC)_8][HPW_{12}O_{40}]$ for NENU-29, $Cu_{12}(BTC)_8$ for HKUST-1$(Cu_3(BTC)_2)$.
[31] J.L.C. Rowsell, O.M. Yaghi, J. Am. Chem. Soc. 128 (2006) 1304–1315.
[32] M. Dincă, J.R. Long, J. Am. Chem. Soc. 127 (2005) 9376–9381.
[33] S.Q. Ma, H.C. Zhou, J. Am. Chem. Soc. 128 (2006) 11734–11735.
[34] B. Chen, X. Zhao, A. Putkham, K. Hong, E.B. Lobkovsky, E.J. Hurtado, A.J. Fletcher, K.M. Thomas, J. Am. Chem. Soc. 130 (2008) 6411–6423.
[35] F. Daniels, J.W. Williams, P. Bender, R.A. Alberty, C.D. Cornwell, Experimental Physical Chemistry, McGraw-Hill, New York, 1962.
[36] R.T. Yang, Gas Separation by Adsorption Processes, Butterworth, Boston, 1997.
[37] X. Lin, A.J. Blake, C. Wilson, X.Z. Sun, N.R. Champness, M.W. George, P. Hubberstey, R. Mokaya, M. Schröder, J. Am. Chem. Soc. 128 (2006) 10745–10753.